Amplifying Waveguide Optical Isolator with Integrated Electromagnet

Wouter Van Parys, Dries Van Thourhout, Roel Baets (1) Beatrice Dagens, Jean Decobert, Odile Le Gouezigou, Dalila Make (2) and Liesbet Lagae (3)
1) Department of Information Technology, Ghent University - IMEC, St-Pietersnieuwstraat 41, 9000 Gent, Belgium (wouter.vanparys@intec.ugent.be) 2) Alcatel Thales III-V Lab, Route Départementale 128, 91767 Palaiseau, France (beatrice.dagens@3-5lab.fr) 3) Interuniversitair Micro-Elektronica Centrum, IMEC vzw, Kapeldreef 75, 3001 Leuven, Belgium (liesbet.lagae@imec.be)

Abstract: *We have demonstrated an amplifying waveguide optical isolator with integrated electromagnet. This provides a solution to the generally poor magnetic remanence of this type of isolator. The proof of principle is presented and optimization routes are discussed.*

Introduction

An optical isolator is indispensable in an optical telecom link to protect semiconductor lasers from optical feedback. A planar, waveguide version of the optical isolator is highly desirable as it would greatly reduce the packaging cost – hence the overall cost – of a laser diode module, because it avoids the expensive alignment required with current commercial bulk isolators.

An integratable isolator configuration that is getting a lot of attention recently is the amplifying waveguide optical isolator [1-4]. The device basically is a semiconductor optical amplifier (SOA) with a transversally magnetized ferromagnetic film close to the guiding core. The magneto-optic (MO) Kerr effect causes a non-reciprocal shift of the complex effective index of the guided modes, implying that the modal loss is dependent on the propagation direction. Current injection decreases the overall loss level in the device. As illustrated in the bottom part of figure 1, the result is a device which, being transparent in one direction while providing loss in the opposite direction, is isolating. The main advantage of this isolator concept is that monolithic integration with a semiconductor laser is straightforward, as both components are essentially the same. Configurations operating in TM-polarization [1, 3-4], illustrated in figure 1 (top), and TE-polarization [2] have been demonstrated in recent years.

One of the main issues for this kind of device is the magnetization of the ferromagnetic metal film. The very high aspect ratio of the length of the film to the width results in very low remanent magnetization of the film due to large demagnetizing fields. One of the solutions to this problem is to have a magnet integrated with the isolator. In this paper we demonstrate an amplifying waveguide isolator with an integrated electromagnet. This magnet is a gold stripe deposited along the longitudinal direction of the isolator in close vicinity of the bias contact. Current flowing from one side of the cavity to the other generates a transverse magnetic field causing the magneto-optic Kerr effect.

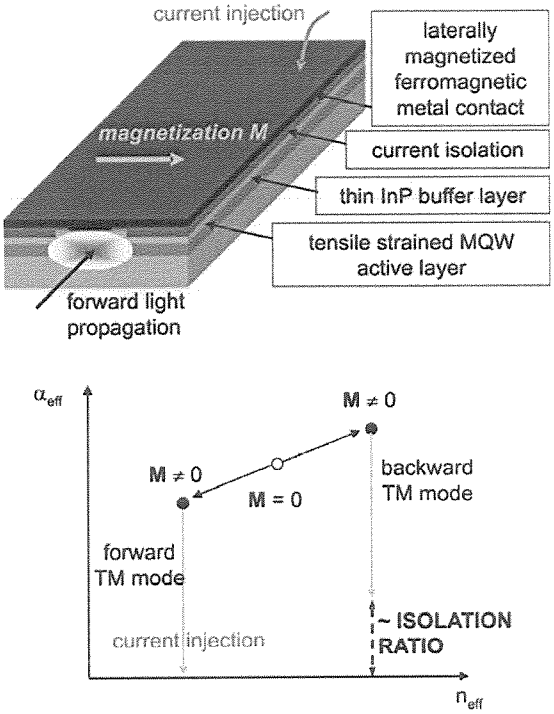

Fig. 1: Lay-out (top) and operation principle (bottom) of the TM-mode amplifying waveguide optical isolator.

Apart from application as an optical isolator, this result is interesting in itself as it is now possible to modify the internal loss of an SOA dynamically and non-reciprocally.

Design

The design of the amplifying waveguide optical isolator and the integrated electromagnet can be considered as two separate parts, which will both be discussed in this paragraph.

The operation of the isolator is determined by the interplay of the source of the non-reciprocal loss shift – the ferromagnetic metal – and the gain that can be provided by the amplifying material to compensate the absorption in the metal film. The optimization of both building blocks has been extensively discussed earlier [4]. The amplifying core is an AlGaInAs (λ_g = 1288nm) tensile strained multiple quantum well

structure, where the built-in tensile strain provides TM-selective material gain while suppressing TE-gain. As was demonstrated by Decobert et al., [5] the gain parameter g_0 can be strongly enhanced by increasing the amount of tensile strain; hence a very large value of -1.6% strain is built-in in the quantum wells. Three Co_xFe_{1-x} compounds have been characterized ($Co_{90}Fe_{10}$, $Co_{50}Fe_{50}$ and Fe) and $Co_{50}Fe_{50}$ was found to be the best compromise between a high MO effect and low absorption [6]. The MO metal film also acts as the electrical contact for the underlying semiconductor optical amplifier. Low contact resistivity combined with minor additional absorption is provided by a hybrid Be p^+-doped $In_{0.81}Ga_{0.19}As_{0.41}P_{0.59}$ / $In_{0.54}Ga_{0.46}As$ bilayer (thickness = 100nm/15nm, $N_{Be} = 2.0\ 10^{19}cm^{-3}$ / $3.0\ 10^{19}cm^{-3}$) [7].

Apart from the two main building blocks the isolator design is a matter of optimization of the thickness of the cladding layers; the two $In_{0.86}Ga_{0.14}As_{0.32}P_{0.68}$ separate confinement heterostructure (SCH) layers surrounding the quantum well core and the InP buffer thickness between the amplifying core and the contact structure. The procedure for the design of these geometric device parameters targets optimization of the practical device specifications. The corresponding figure of merit to be minimized is the total bias current required for transparency in the forward propagation direction corresponding to 1dB of optical isolation. The 1D simulations have been done with an optical mode solver [8] extended with a perturbation-based algorithm for MO waveguide calculation [9]. A steepest-descent algorithm was implemented to obtain the best values for the three geometric parameters. Theoretically, the isolator has a FoM equal to 7.45mA/dB isolation for a ridge width of 2μm, and a cavity length of 155μm/dB isolation.

A schematic cross-section of the amplifying waveguide optical isolator with integrated electromagnet is given in the top part of figure 2. The design parameters for the electromagnet are the width of the gold stripe and the distance between the electromagnet and the ferromagnetic metal film. Other parameters are the thickness of the gold stripe, which influences the current density in the electromagnet but not the strength of the magnetic field, and the variation of the generated magnetic field in the lateral direction (x-direction), which is of only minor importance if the stripe width is much larger than the width of the ferromagnetic film. It is to be noticed that the-latter has to be the case for the isolator to ensure that the magnetic field is aligned along the lateral direction (x-direction).

The partial differential equation describing the magnetic field problem was solved with MATLAB. The bottom part of figure 2 shows the result of these calculations. The simulated values of the magnetic flux density (in mT) are plotted for variation of the width of the electromagnet and the distance from the electromagnet per unit (mA) current injection in the gold

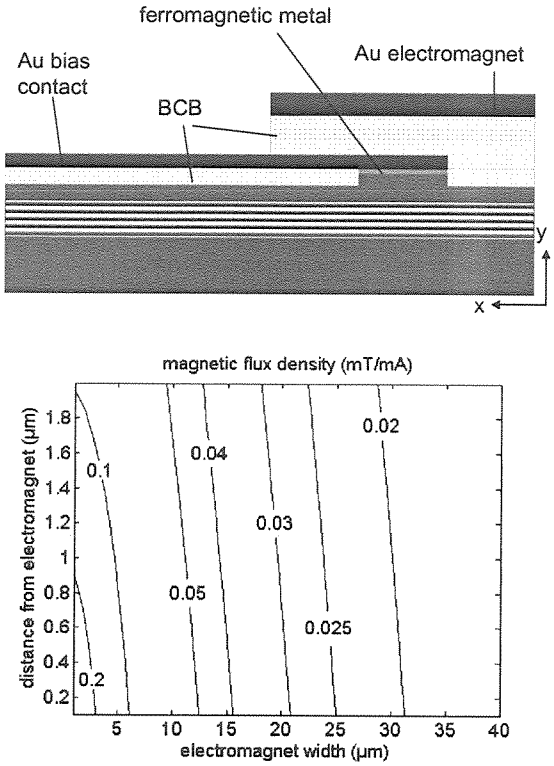

Fig. 2: (top) Schematic cross-section of the amplifying waveguide isolator with integrated electromagnet. (bottom) Simulation of the lateral magnetic flux density (x-direction) as a function of the width of the electromagnet gold stripe and the distance (y-direction) from the electromagnet, expressed in mT per mA of current injection.

stripe. For sufficiently wide stripes the generated magnetic field is quasi-independent of the distance from the electromagnet. This is an advantage for the fabrication because the use of a thick separation layer between bias contact and electromagnet reduces the risk of short-circuiting both metal layers.

With the available lithography mask it was only possible to have an electromagnet gold stripe as wide as 30μm, resulting in a magnetic field that is far from optimized. However, it is suitable for the first demonstration of the principle.

Fabrication

The isolator was grown with metal organic vapor phase epitaxy on an n^+ S-doped InP substrate ($N_S = 3.0\ 10^{18}cm^{-3}$). The layer structure is a Si n-doped ($N_{Si} = 10^{18}cm^{-3}$) InP cladding layer, the non-intentionally doped (n.i.d.) optimized active core, a Be p-doped InP cladding ($N_{Be} = 5.0\ 10^{17}cm^{-3} \rightarrow 2.0\ 10^{18}cm^{-3}$) and the optimized contact structure. The sputter-deposited 50nm thick $Co_{50}Fe_{50}$ film, capped with a 40nm/150nm Ti/Au protective bilayer, was patterned into 2μm wide stripes with standard lift-off. Ridge waveguides were defined with CH_4:H_2 plasma reactive ion etching using these metallic stripes as an etch

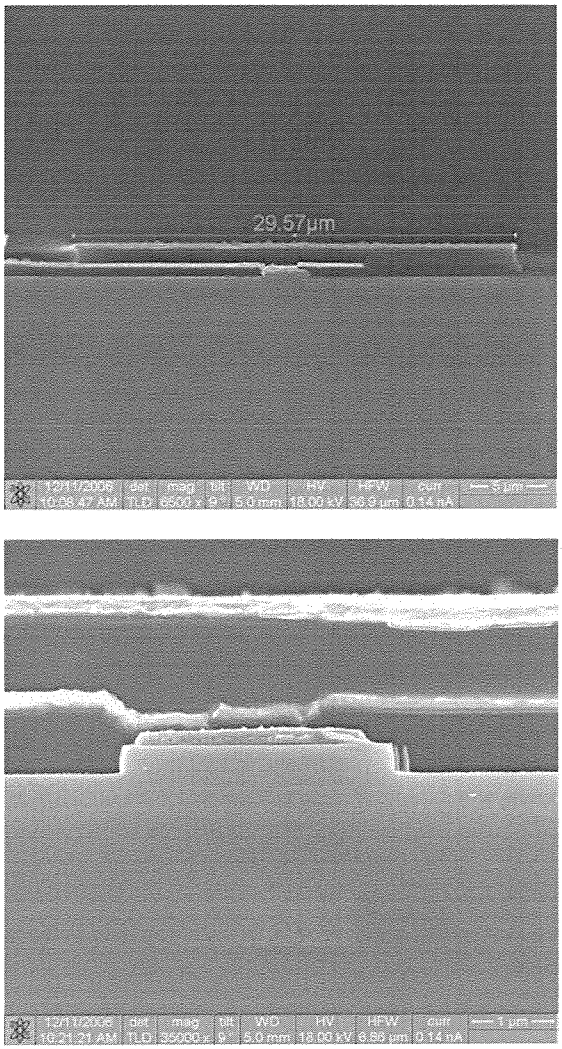

Fig. 3: SEM pictures of the cross-section of the amplifying waveguide optical isolator with integrated electromagnet.

mask. With this technique full covering of the ridge with metal has been achieved. An additional 30µm wide gold stripe is evaporated to enable contacting of the isolator, separated from the semiconductor surface by a benzocyclobutene (BCB) current isolation layer. On top of the isolator bias contact a 30µm wide and 250nm thick gold stripe is deposited, serving as the electromagnet. Both gold stripes are separated by a 1µm thick BCB layer. Isolators with a cavity length of 1.3mm have been cleaved and mounted for characterization.

In figures 3 two scanning electron microscope (SEM) images of a cross-section of the amplifying waveguide optical isolator with integrated electromagnet are given. The top picture shows that the fabricated device is in agreement with the design. When zooming in on the ridge waveguide (bottom part of figure 3) it can be seen that the definition of the ridge is not perfect, with a ridge width that is slightly wider than designed roughness present at the side of the

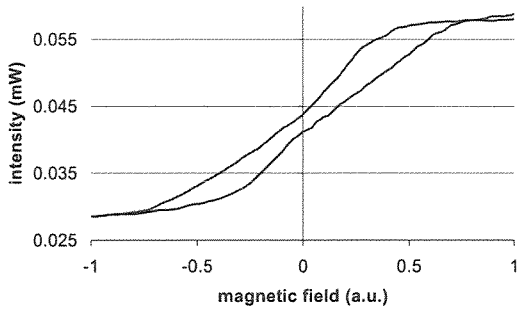

Fig. 4: Optical power emitted by the optical isolator as a function of the externally applied magnetic field at a bias current of 140mA (= above threshold).

ridge. However, these inaccuracies are not expected to influence the operation of the integrated electromagnet.

Characterization

As was previously elaborated [10] an easy and fast characterization method for the amplifying waveguide optical isolator is to pump as-cleaved isolators above threshold and extract the emitted power as a function of the applied lateral magnetic field – switching the magnetic field direction is equivalent to switching the light propagation direction. Because the material gain is clamped above threshold the non-reciprocal loss shift is independent of the isolator bias current and the optical isolation can be extracted from the ratio of forward to backward intensity – or equivalently the intensity at magnetization in either lateral direction:

$$isolation\,[dB] = \frac{10}{ln\,10}\,2\,ln(intensity\ ratio) \qquad (1)$$

In order to evaluate the performance of the integrated electromagnet, the amplifying waveguide isolator was initially characterized with an external electromagnet. In figure 4 the emitted power is plotted as a function of the externally applied magnetic field for a bias current of 140mA on a 1.3mm isolator. The corresponding maximal isolation, at saturation magnetization, is 6.1dB. This graph shows that the remanent isolation – at zero magnetic field – is only 8.5% of the maximum value.

Next, the integrated electromagnet was characterized by applying current to the gold strip while pumping the isolator above threshold. To avoid heating, the electromagnet is driven with pulsed current (pulse width 0.3µs, duty cycle 3%). The isolator bias current is continuous wave (CW). The output signal is evaluated on an optical oscilloscope. The measurement is done for both directions of the current flow in the electromagnet, corresponding to a magnetic field in either lateral direction. The bottom part of figure 5 shows the measured intensity time evolution corre-

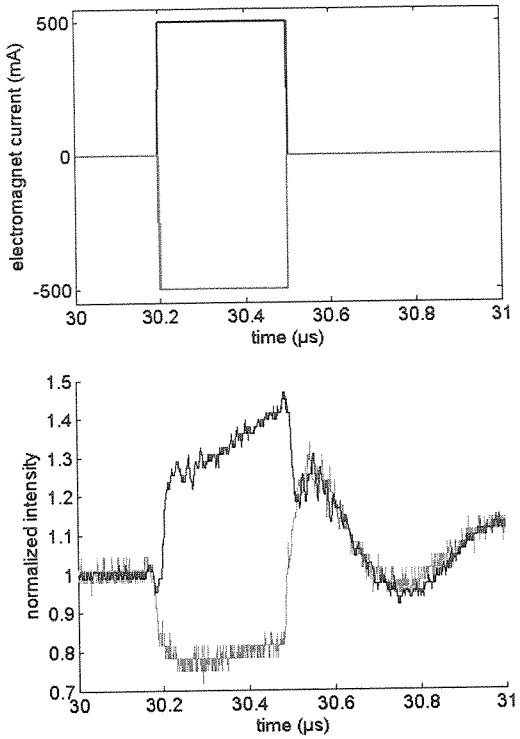

Fig. 5: (top) Time evolution of the injected (pulsed) current in the electromagnet. (bottom) Corresponding (normalized) intensity emitted by the amplifying waveguide optical isolator at a bias current of 140mA (= above threshold).

sponding to the pulsed current of figure 5 (top), where negative current corresponds to reversed current flow direction. The intensity is normalized to compensate for variations in the fiber-to-chip coupling. At the on-set of the current pulse the emitted power rapidly increases or decreases, depending on the current flow direction. This is a clear proof of the on-set of the non-reciprocal loss shift. After the off-set of the pulse, the emitted power quickly becomes identical again in both cases and then slowly recovers from the heating of the device. The ratio of the intensity at "forward" to that at "backward" current injection equals 1.64, which for an isolator of 1.3mm cavity length corresponds to an isolation of 4.3dB, or 70% of what is achieved at saturation magnetization.

We repeated the measurements for different values of the electromagnet current injection. In figure 6 the corresponding evolution of the optical isolation with injected (pulsed) current is plotted. For comparison the optical isolation as a function of the strength of an externally applied magnetic field is also given. From this graph it can be derived that with a current injection of 500mA the achieved magnetic field is about half the value needed to saturate the ferromagnetic film.

The results in figure 6 shows that a very high current of 1.1A is needed to achieve magnetic saturation with the fabricated electromagnet. However, as previously

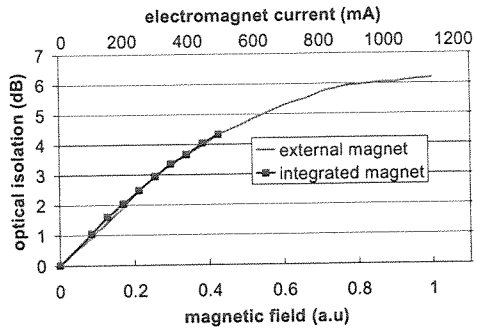

Fig. 6: Evolution of the optical isolation with injection current in the electromagnet and with externally applied magnetic field.

mentioned, due to limitations in the fabrication the demonstrated electromagnet design is far from optimized. Adjusting the width of the gold stripe will decrease the required current by at least a factor of 5. Furthermore, modification of the ferromagnetic film might decrease the magnetic field – hence the current level – required to saturate the film, a point which needs further investigation.

Conclusion

We have developed an optical isolator with integrated electromagnet. While the demonstrated drive current is beyond the acceptable level, possibilities for major improvement have been identified. Decrease of the required current injection should also enable CW operation of the electromagnet.

Acknowledgment

This research was partially performed in the frame of the European Union IST-project ISOLASER.

References

1 M. Vanwolleghem et al., APL, **85**, 3980 (2004).
2 H. Shimizu et al., JLT **24**, pp.38-43 (2006).
3 V. Zayets et al., APL, **86**, 261105 (2005).
4 W. Van Parys et al., APL, **88**, 071115 (2006).
5 J. Decobert et al., J. Crystal Growth **272**, 542 (2004).
6 M. Vanwolleghem et al., JOSA B **24**, p.94-105 (2007).
7 W. Van Parys et al., 2006 LEOS Annual Meeting (Montreal), p.679-680 (2006).
8 P. Bienstman et al., Opt. and Quant. Elect. **33**, 327-341 (2001).
9 K. Postava, et al. JOSA B **22**, 261-273 (2005).
10 W. Van Parys et al., ECIO 2005 (Grenoble), p.33-36 (2005).

Conference Proceedings

European Conference on Integrated Optics

and Technical Exhibition

ECIO 2007

COPENHAGEN DENMARK APRIL 25-27

Modelling
Sensors
Fabrication
Nanophotonics
Characterisation
Bio-medical applications
Hybridisation
Microphotonics
Applications
Communication

Organised in conjunction with **OWTNM 2007**
Workshop on
Optical Waveguide Theory and Numerical Modelling
April 27-28, 2007